

Polarisation of radio waves transmitted through Brunt Ice Shelf

C S M Doake and H F J Corr

*British Antarctic Survey, Natural Environment Research Council
Madingley Road, CAMBRIDGE CB3 0ET, UK*

Abstract

The polarisation behaviour of radar waves transmitted through Brunt Ice Shelf at a site near Halley has been investigated using a step-frequency radar with a centre frequency of 300 MHz and a bandwidth of 150 MHz. Two linearly polarised aerials were used. At nine different orientations of the transmitting aerial, data were collected for nine different orientations of the receiving aerial, both covering a 180° rotation. This is the first study in which both phase and amplitude data have been analysed to determine the birefringence of the ice, which is related to the crystal fabric. The anisotropy in the effective permittivity is found to be about 0.14%, about a quarter of that found on Bach Ice Shelf with a 60 MHz radar in 1977.

Introduction

Single crystals of ice are known to be birefringent at optical frequencies due to the anisotropy in the permittivity (about 0.2%). Naturally occurring ice, I_h , has hexagonal symmetry, and is uniaxial with the optic axis coinciding with the crystallographic c -axis. It is optically positive, so that the ordinary ray has a higher velocity than the extraordinary ray that travels along the slow, or optic axis. The anisotropy in the permittivity is around 1.1% in the HF, VHF and microwave frequency ranges (Fujita et al, 1993; Matsuoka et al, 1997).

In an ice sheet, the polycrystalline nature of the ice means that the effective birefringence is determined by the average crystal fabric (Hargreaves, 1978; Fujita and Mae, 1993). A strongly aligned fabric will lead to a strong birefringence. Fabrics evolve to develop characteristic patterns depending on the deformation history (Castelnau et al, 1996), so that, for example, near the bed of an ice sheet not too far from a divide there will often be a strong single axis fabric, orientated with the c -axis vertical.

Since ice sheets were first sounded by radar, it has been known that they affect the polarisation of radio waves (Jiracek, 1967). However, the few systematic studies that have been carried out have analysed only echo strength, not phase, and have come up with limited results (Hargreaves, 1978; Woodruff and Doake, 1979; Yoshida et al, 1987; Fujita and Mae, 1993). Most studies have treated the phenomenon as a curiosity. The implications have been largely ignored for normal ice sounding, despite the variation of more than 20 dB in echo strength that can result from different antenna orientations.

A simple technique for determining polarisation parameters will give a powerful tool for mapping ice fabrics, which will give a new perspective on fabric evolution and understanding the deformation history and dynamics of ice sheets. In a preliminary study for an advanced radar for BAS, we collected data with an HP network analyser, configured as a step-frequency radar, near Halley on Brunt Ice Shelf on 6 February 1999 to examine the polarisation behaviour of radio

waves in ice. The radar had an effective centre frequency of 300 MHz and a bandwidth of 150 MHz. Using separate transmitting and receiving aerials, the transmitter was placed at one orientation and the receiver rotated a full 180 degrees, in nine separate steps at orientations of 0, 30, 45, 60, 90, 120, 135, 150 and 180 degrees from a line bearing 120 degrees true. This was repeated for the same nine different orientations of the transmitter giving a total of 81 separate readings. The aerials were turned by hand and the error in aligning them is probably less than 5 degrees. The matrix of results shows that there is close correspondence between transmitting and receiving aerials – similar values are obtained by transmitting at a given angle while receiving at another, and with swapping the transmitting (Tx) and receiving (Rx) aerials orientations. This is expected from the concept of reciprocity of aerials, a basic tenet of antenna theory. Each reading took just over a minute to complete, so that the complete experiment lasted about two hours.

Data analysis

Amplitude data were analysed using Equation 13 of Doake (1981):

$$|E_{\theta}|^2 = E_0^2 R_x^2 (\cos^2 \beta \cos^2 \theta + r^2 \sin^2 \beta \sin^2 \theta + 0.5r \sin 2\beta \sin 2\theta \cos \delta) \quad (1)$$

where E_{θ} is the field intensity measured in a receiving aerial at an angle θ to the x-axis, β is the angle of the transmitting aerial to the x-axis, δ is the phase difference between the ordinary and extraordinary rays (i.e. the phase shift introduced by the birefringence of the ice, whose optic axis is aligned along the y-direction), E_0 the intensity of the transmitted wave and R_x the resulting attenuation due to propagation and reflection. Both aerials are assumed to be linearly polarised. The ratio between the attenuation in the x direction, R_x and the y-direction, R_y , is given by $r=R_y/R_x$. We expect δ to be determined mainly by the birefringence of the ice and r by the reflecting surface, although there may be cross contributions. The horizontal measurement reference frame (x' , y'), used in the field to orientate the transmitting and receiving aerials, is aligned at an angle ϵ to the x-axis, as shown in Figure 1.

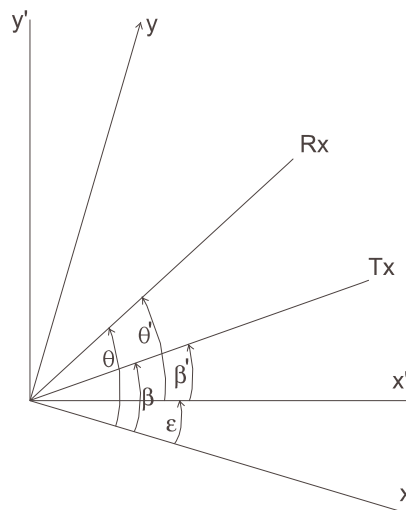


Figure 1. Coordinate axes for

polarisation measurements.

The relationship between the angles β and θ and the reference frame is given by:

$$\beta = \beta' + \epsilon$$

$$\theta = \theta' + \varepsilon$$

Substituting these expressions in Equation (1) gives an equation containing the unknowns to be solved for: ε , δ and r . The observations give E_θ as a function of β' and θ' .

Equation 1 describes the shape of the power measured as a function of Rx and Tx orientations. For a constant Tx angle (β'), rotating the receiver (varying θ') draws out a dumb-bell shape in polar coordinates (Figure 2), assuming the power for angles 180 to 360 is the same as 0 to 180. Figure 2 also shows that keeping the Rx orientation constant and rotating the transmitter gives very similar results.

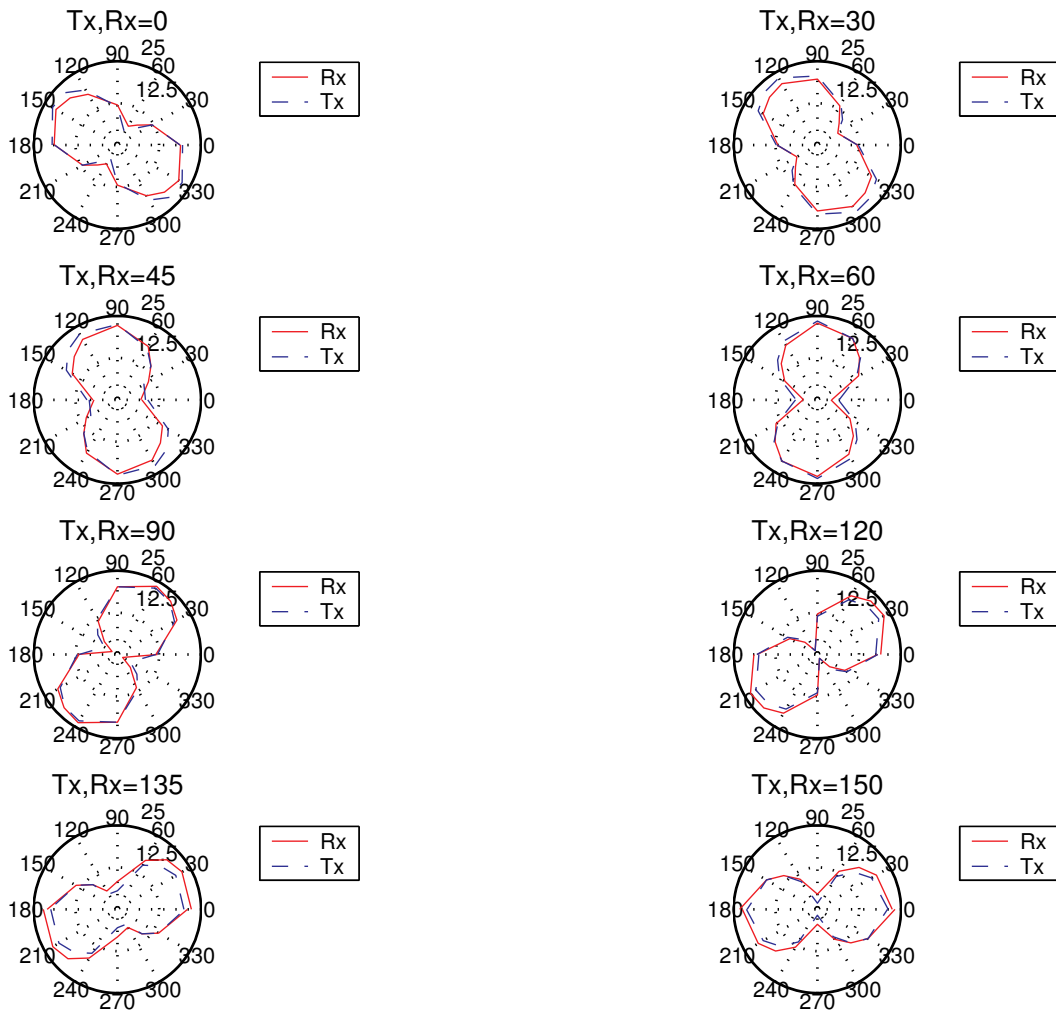


Figure 2. Variation of amplitude obtained by rotating either the receiving or transmitting aerial.

The maximum power is received at receiver angle θ'_{\max} . Plotting θ'_{\max} against transmitter angle β' allows the direction of the optic axis to be determined by $\theta'_{\max} = \beta'$ (when both Rx and Tx lie along the y-direction). Figure 3 shows the behaviour of θ'_{\max} v β' for various values of δ (note that the same curve is obtained for δ and $-\delta$). The magnitude of the phase shift can be estimated as less or greater than 90° by the rotation behaviour - whether or not θ'_{\max} and β' rotate in the same or opposite senses, respectively.

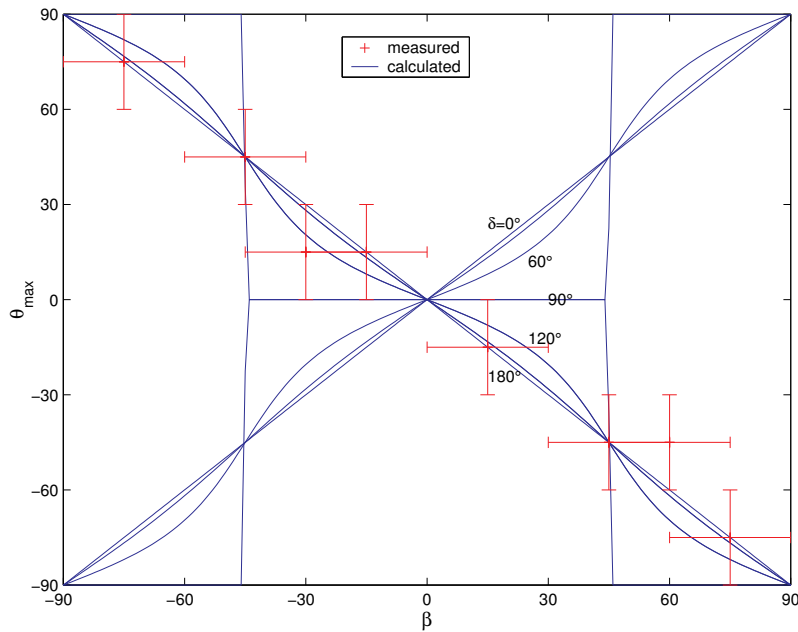


Figure 3. Plot of θ_{max} v β , showing opposite sense of rotation when $90 < \delta < 270$.

The variation with transmitter angle of the sum of the powers received in crossed dipoles (Figure 4) can be used to determine the value of r (Doake, 1979), and was found to be 1.07 ± 0.03 .

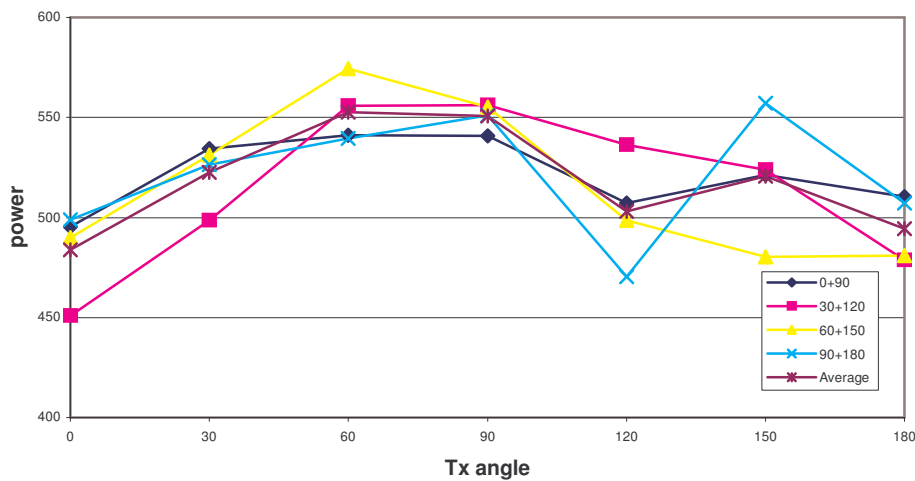


Figure 4. Sum of powers received in crossed dipoles.

Polarisation results collected using parallel transmitting and receiving aerials (Hargreaves, 1977; Fujita and Mae, 1993) have been interpreted using equation (1) with $\beta = \theta$, which reduces to Equation (17a) in Doake (1981). We can simulate this configuration by taking the diagonal terms in the matrix of amplitude observations and assuming a negligible unpolarised component. An optimisation method searching the parameter space occupied by the three unknowns (ϵ , δ , r) with a resolution of (1° , 1° , $.01$) gives the best-fit values of (15° , 151° , 1.12). The resulting fit is shown in Figure 5. There was a 24 dB difference between the greatest and least power for parallel receiving and transmitting aerials (i.e. for the power which would be received by a single antenna transmit-receive system).

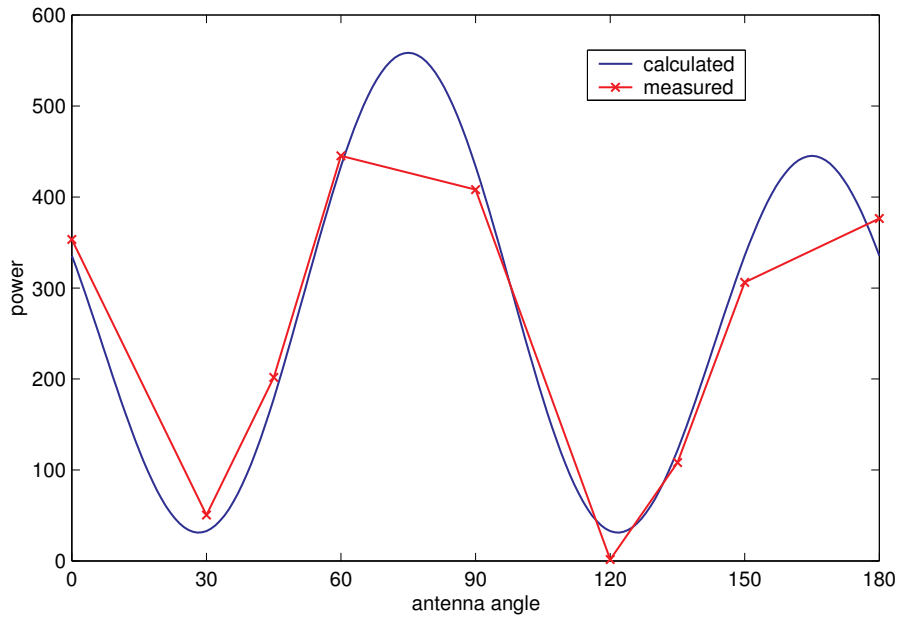


Figure 5. Comparison between measured and calculated powers for parallel transmitting and receiving aerials.

Phase measurements

The phase difference ϕ between the field E_x measured along the x-axis and the field E_θ measured at an angle θ to the axis can be found from the expression (Doake, 1981)

$$\tan \phi = \frac{\tan \alpha \tan \theta \sin \delta}{1 + \tan \alpha \tan \theta \cos \delta}$$

but used in the form

$$\tan \phi = \frac{r \sin \beta \sin \theta \sin \delta}{\cos \beta \cos \theta + r \sin \beta \sin \theta \cos \delta}$$

in order to resolve ambiguities in the value of ϕ which arise from the former expression. Here, $\tan \alpha = E_{y0}/E_{x0} = r \tan \beta$ expresses the relationship between the orientation of the transmitter to the x-axis (β) and the ratio of the amplitudes of the electric field components (E_{y0}/E_{x0}) which describe the polarisation ellipse (Doake, 1981). To make the theoretical curves fit the measured values, 2π has had to be added to some values and an offset (representing the absolute phase along the x-axis) also applied (Figure 6). An optimisation technique on all the phase measurements gives the best estimates of (ϵ, δ, r) as $(13^\circ, 150^\circ, 1.17)$ with a resolution of $(1^\circ, 1^\circ, .01)$, in good agreement with estimates from the power analysis of $(15^\circ, 151^\circ, 1.12)$.

Optimisations were carried out on a number of subsets of the phase measurements, such as transmitting and receiving at only three or four orientations, to estimate how accurately the birefringence parameters could be measured. These results suggest that ϵ was $15^\circ \pm 2^\circ$, the value of δ was $145^\circ \pm 10^\circ$, and r was 1.1 ± 0.1 .

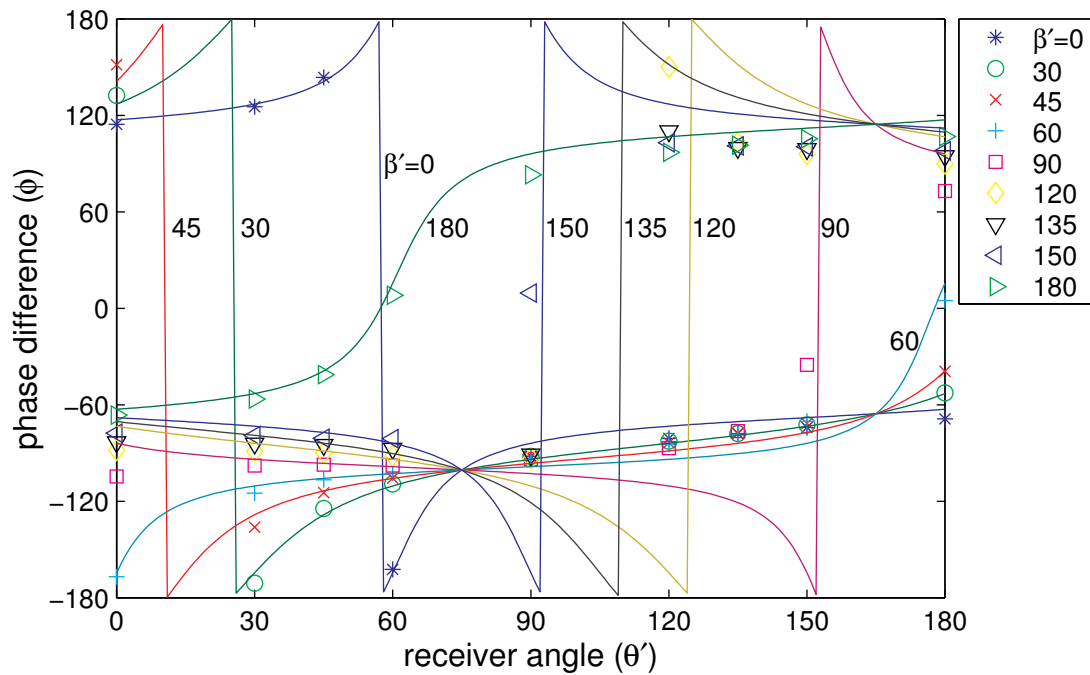


Figure 6. Comparison between measured (symbols) and calculated (lines) values of the phase difference, using 'best-fit' values with optic axis at 75° ($\epsilon=15^\circ$), $r=1.1$, $\delta=145^\circ$.

Birefringence

Using the relationship connecting the phase change introduced by the passage of the radio waves through the ice, the difference in the refractive index for the ordinary and extraordinary waves, and the ice thickness:

$$\delta = 2\pi/\lambda (n_E - n_O)H$$

where H is ice thickness, λ the wavelength in air, δ the phase difference, n the refractive index ($=\sqrt{\epsilon}$), then

$$\Delta n = \delta\lambda/4\pi H$$

and $\Delta\epsilon/\epsilon = 2\Delta n/n = \delta\lambda/2\pi Hn$. Taking $\epsilon = 3.17$ (i.e. $n = 1.78$) for ice gives the following table comparing the results from Brunt Ice Shelf with those found on Bach Ice Shelf, on the Antarctic Peninsula (Woodruff and Doake, 1979).

Site	δ (degrees)	λ (m)	H (m)	Δn	$\Delta\epsilon/\epsilon$
Brunt Ice Shelf	150	1	170	1.2×10^{-3}	0.14%
Brunt Ice Shelf	150+360	1	170	4.2×10^{-3}	0.47%
Bach Ice Shelf	180	5	270	4.6×10^{-3}	0.52%

This gives the minimum value for the anisotropy, as there could be additional phase differences of $2n\pi$ in the polarization. So, either the anisotropy on Brunt Ice Shelf (at Halley) is about 1/4 that on Bach Ice Shelf, or if the anisotropy is the same, there is an extra 2π in the phase difference. The lower value would represent about 10% of the maximum anisotropy of a single ice crystal, suggesting a well-formed but relatively weak fabric at Halley.

The optic axis lies at an angle of 75 ± 2 degrees from the reference line, i.e. on a bearing of $45^\circ - 225^\circ$ true (north east – south west). For comparison, the velocity vector at Halley is almost due west (270° true).

References

- Castelnaud, O, Thorsteinsson, Th., Kipfstuhl, J., Duval, P. and Canova, G.R. 1996. Modelling fabric development along the GRIP ice core, central Greenland. *Annals of Glaciology*, 23, 194-201.
- Doake, C.S.M. 1979. Characterizing the glacier bed using a radio-echo technique. *Journal of Glaciology*, 23(89), 404.
- Doake, C.S.M. 1981. Polarization of radio waves in ice sheets. *Geophysical Journal of the Royal astronomical Society*, 64, 539-558.
- Fujita, S. and Mae, S. 1993. Relation between ice sheet internal radio-echo reflections and ice fabric at Mizuho Station, Antarctica. *Annals of Glaciology*, 17, 269-75.
- Fujita, S., Mae, S. and Matsuoka, T. 1993. Dielectric anisotropy in ice Ih at 9.7 GHz. *Annals of Glaciology*, 17, 276-280.
- Hargreaves, N.D. 1977. The polarization of radio signals in the radio echo sounding of ice sheets. *Journal of Physics. D Applied Physics*, 10(9), 1285-1304.
- Hargreaves, N.D. 1978. The radio frequency birefringence of polar ice. *Journal of Glaciology*, 21, 301-313.
- Jiracek, G.R. 1967. Radio sounding of Antarctic ice. *University of Wisconsin Geophysical and Polar Research Centre, Research Report Series No. 67*, 1-127.
- Matsuoka, T., Fujita, S., Morishima, S. and Mae, S. 1997. Precise measurement of dielectric anisotropy in ice Ih at 39 GHz. *Journal of Applied Physics*, 81(5), 2344-48.
- Woodruff, A.H.W. and Doake, C.S.M. 1979. Depolarisation of radio waves can distinguish between floating and grounded ice sheets. *Journal of Glaciology*, 23(89), 223-232.
- Yoshida, M., Yamashita, K. and Mae, S. 1987. Bottom topography and internal layers in East Dronning Maud Land, East Antarctica, from 179 MHz radio echo-sounding. *Annals of Glaciology*, 9, 221-224.